www.nature.com/scientificreports

scientific reports

OPEN

Real time response strategy for reservoir storage maintenance and desiltation operations

Cheng-Chia Huang[1] & Fong-Zuo Lee[2]✉

Taking a representative reservoir storage conservation area, Taiwan as an example, the average volume of sediment accumulated in reservoirs has reached one-third of the original designed capacity. This has posed challenges to the utilization of water resources. Therefore, understanding the behavior of sediment transport into reservoirs is crucial for effective reservoir desilting operations. This study applies a practical turbidity current model to investigate the variations in velocity and sediment concentration during the transport of turbid inflows within the reservoir. This enables the estimation of sediment discharge at various outlet works and facilitates the optimization of sediment flushing strategies. The model is validated through numerical simulations based on historical typhoon events. Then, proposes a three-stage approach, including the travel pattern, the updated operation suggestion, and the economic evaluation to combine a cost analysis utilizing mechanical dredging and public water supply employed as a principal countermeasure. Most importantly, this research presents the most convenient and cost-effective way of managing reservoir water resources to take care of both desilting and storage during typhoons. Additionally, the preliminary concept is proposed that real-time prediction can be developed in the field reservoir by using the numerical method in the future.

Keywords Water resources, Desilting operation, Turbidity current model, Principal countermeasure

Reservoir sedimentation is a critical challenge worldwide, significantly impacting water storage capacity, flood control, and hydropower generation. The continuous accumulation of sediment reduces reservoir lifespan and threatens sustainable water resource management. This study aims to grasp the sedimentation processes and formulate a proper release strategy to mitigate reservoir deposition effects. Resisting the sediment flow into the reservoir zone is a common approach; check dams are often built upstream of the reservoir to decrease sediment inflow proportion and maintain reservoir storage capacity[1–3]. Dredging is regarded as a removal approach that excavates sediment from the reservoir during regular periods, except during typhoons, and slightly extends the reservoir lifespan[4–6]. The construction of a bypass tunnel is considered a suitable sediment release strategy to operate during typhoons because the sediment could be passed through the tunnel to the downstream river and avoid the sediment deposit on the reservoir bed[7–9]. Note that these approaches are often applied in field reservoirs to prolong reservoir life. However, a common feature is that these methods need time, manpower, and investment. For example, check dams sometimes are insufficient to store sediment, and deposited sediment has to be removed to maintain the sediment trap ability of the dam; bypass tunnel construction requires a large amount of money and time, and maintenance fees have to be considered after it operates; the dredge engineering have the manpower, and environmental issues, the removing efficiency often insufficient to follow the reservoir deposition rate[10,11].

Technical speaking, the function of the existing reservoir outlet not only includes water level adjusting, agricultural irrigation, and hydropower generation but also can be further operated to release inflow sediment during flooding[12–17]. Notably, the sediment transportation pattern significantly differs between the mountain river and the reservoir area. The typhoon event causes enormous runoff; an approaching supercritical flow could happen from upstream. Finally, the hyper-concentration fluid transforms to the subcritical flows in the reservoir due to the deep water and broad cross-section[18,19]. Most importantly, the subcritical flow will further convert into a unique flow pattern because the hyper-concentration material contacts the surrounding water in the reservoir, and the density matches the plunge condition to produce it, the turbidity current flow. Besides, the inflow material generates a significant interface between upper water and downer sedimentation when it passes through the plunge point. A double-layer flow emerges and moves to the dam front[20–22]. Undoubtedly,

[1]Department of Water Resources Engineering and Conservation, Feng Chia University, Taichung City 407102, Taiwan (R.O.C.). [2]Department of Civil Engineering, National Chung Hsing University, Taichung City 402202, Taiwan (R.O.C.). ✉email: fzlee@nchu.edu.tw

understanding the movement of turbidity current is an important topic in providing sediment release timing for reservoir management. Adopting a practical tool to conduct the turbidity current flow investigation is the primary mission, and the related references are shown below.

Collecting the measurement data is a direct way to investigate the density current flow. The travel pattern, sediment concentration, and material amount of turbidity were adopted in different papers, and the research results can be provided for the calibration and validation data of other tools[23–28]. The physical model is a widely adopted approach to grasp the turbidity current flow. The flume experiment or the down-scale model often be applied to understand the flow pattern of the turbidity current. Sediment desilitation can be formulated using the experiment outcome to maintain reservoir sustainability[20,29–32]. Apart from the measurement methods and physical model, the numerical model is technically regarded as a consistent and practical analysis approach for turbidity current flow. Additionally, the 2-D model is considered a suitable model for studying the turbidity current flow of the field reservoir, because it includes the advantages of the simulation efficiency from the 1-D model and the accuracy from the 3-D model[33–38].

While 3D models provide higher accuracy in capturing vertical variations, the 2D layer-averaged model remains widely used in reservoir studies due to its computational efficiency and practicality in large-scale simulations. Previous studies have demonstrated that the 2D model effectively captures the horizontal movement of turbidity currents, which is the primary focus of this study. Such as, Hu et al.[39] adopted the 2-D turbidity currents model to investigate the turbidity current transport rate in the field site reservoir. The results indicated that it could be a valuable tool for operating the sluice gates to release excess sediment from the reservoir. Huang et al.[40] and Lee and Huynh Nguyen[41] found that the 2-D model is capable of predicting the movement of turbidity current toward the dam face and the sluicing out of outlets at different elevations and is valid and practical for field applications. The study also established guidelines for suitable sensitivity parameter ranges in the field site and presented that the mesh size and drag coefficient are crucial parameters that need to be taken into consideration. Anari et al.[42] indicated that the 2-D model is appropriate for simulating the horizontal movement of the turbidity current, especially the release behavior near the reservoir sluice gates. The most important is that considering sediment transportation in reservoir management is crucial for ensuring reservoir storage sustainability.

Above all, a numerical model is a proper tool for studying turbidity current behavior, including the flow pattern, sediment concentration, and releasing amount. Note that the 2-D model incorporates the computing efficiency of the 1-D and simulating accuracy of the 3-D model. It can be adapted to help reservoir management grasp the dynamics of turbidity currents and make informed decisions to maintain the reservoir storage capacity. This study focuses on the practical reservoir operation in a field area to simulate the turbidity current characteristic and formulate suitable sediment treatment strategies. Firstly, the moving velocity of the turbidity current needs to be addressed to grasp the current location; the inflow discharge and sediment concentration are determined as crucial factors and discussed below. Then, the releasing ability of different sluice gates is another critical topic. This study presents the reasonable sediment releasing amount results during different historical typhoons to further prove the simulation is creditable to apply to formulate the proper desiltation strategy. The operation timing of the sluice gate is a critical issue for achieving sufficient releasing efficiency. The proper timing should consider the turbidity current movement to operate the sluice gate, and the inflow sediment can be released to maintain the reservoir ability. The most important is that the turbidity current transportation could be predicted, and formulate an appropriate sluice gate operation approach to take care of both reservoir desiltation and water supply during flood duration based on the guideline rule and value presented in this research. Note that the current reservoir operation method focuses on reservoir desiltation or water storage, but challenging to consider both of them. This study aims to develop a real-time response approach for reservoir sediment management by utilizing a turbidity current numerical model. The proposed approach makes three major contributions:

(i) Developing a real-time response system that integrates historical data with numerical models, enabling adaptive sediment management;
(ii) Proposing an optimized turbidity current release strategy that balances sediment flushing and water conservation during extreme hydrological events;
(iii) Introducing a cost-effective framework that combines mechanical dredging with hydraulic desilting, providing a practical and scalable solution for reservoir sediment management.

By bridging the gap between numerical modeling and real-time sediment management, this study provides a practical approach for improving reservoir desiltation efficiency, extending reservoir lifespan, and ensuring sustainable water resource utilization.

Methods
Study area
The idea of building a dam to store water resources in the Shihmen Gorge has existed since 1902 and started construction in July 1956 then lasted 8 years and was officially completed. Shihmen Reservoir is a multi-functional reservoir located in Taoyuan City, Taiwan, East Asia, and operated in 1964. The total length of the Shihmen Reservoir is 16.2 km, and the watershed area is 763.4 km^2. Although the original design capacity of the reservoir was about 309 million m^3 which ranked 3rd storage capacity in Taiwan, observations during several serious typhoon events have proven that the lifespan of Shihmen Reservoir has been overestimated. The original estimated deposition amount should be 48 million and now is two times overreach to 101 million m^3.

There are six major sluice gates for various functions: spillway, spillway tunnel, Shihmen canal, power generation intake, modification tunnel, and permanent river outlet. The specific description shows below, and the location and information as shown in Fig. 3. (i) spillway: the purpose of the spillway is to release the inflow discharge to prevent the dam break during the typhoon period. In addition, the current outflow discharge is 11,400 m^3/s.; (ii) spillway tunnel: the concept of the spillway tunnel was a response to the massive flooding, which threatened the safety of the dam; two parallel drainage tunnels were added in 1984. The outflow discharge of the spillway tunnel is 2400 m^3/s; (iii) Shihmen canal: the Shihmen Canal is a vertical tower-shaped structure that enters the downstream channel system through the gate chamber. It supplies downstream irrigation and domestic demand. The maximum discharge flow rate of the Shihmen Canal is 18.4 m^3/s; (iv) power generation intake: the power generation intake is a 4.5-m-diameter steel pipe. It supplies downstream irrigation and domestic demand. The outflow discharge of the power generation intake is 56 m^3/s; (v) modification tunnel: the modification tunnel is a dedicated pipe modified from the pressure steel pipe of power generation tunnel No. 2. This tunnel can be used to release sediment during typhoon season because the maximum outflow discharge reaches 300 m^3/s; (vi) permanent river outlet: the main function of the permanent river outlet is to discharge water to supply the Taoyuan Canal and part of downstream irrigation areas. It can also be operated to release inflow material during typhoons. The maximum outflow discharge is 34 m^3/s. Note that, the sediment particle needs to be mentioned because particle size plays a crucial role in determining the transport patterns of turbidity current in reservoirs. Technically, coarse particles with higher settling velocities tend to deposit near or upstream of the reservoir entrance, whereas fine-grained sediments remain suspended and travel farther downstream. Hence, the simulation focuses on the fine sediment between 0.01 and 0.02 mm. Besides, TDR (Time Domain Reflectometry) has been applied to the sediment monitoring for the whole-journey of typhoon events[43]. There are 6 observation section are located along the reservoir also shows in Fig. 1.

Study case

The data collection covers 15 typhoon events during the recent decade, and the information includes the flood control operation and sediment releasing operation data of Shihmen Reservoir from 2013 to 2022. A significant trend is presented that the releasing proportion can overreach 30%, the highest is 37.2%, in most of the severe typhoon events, for example, Typhoon Trami, Soudelor, and Dujuan (peak discharge were over 3000 m^3/s), and the lower releasing proportion is shown in moderate and slight typhoons from 1.1 to 27.2%. However, trapped sediment still accounts for more than 60% of the total inflow sediment. Note that reservoir monitoring was conducted in the past decade, and the measured data was often interrupted by environmental issues and

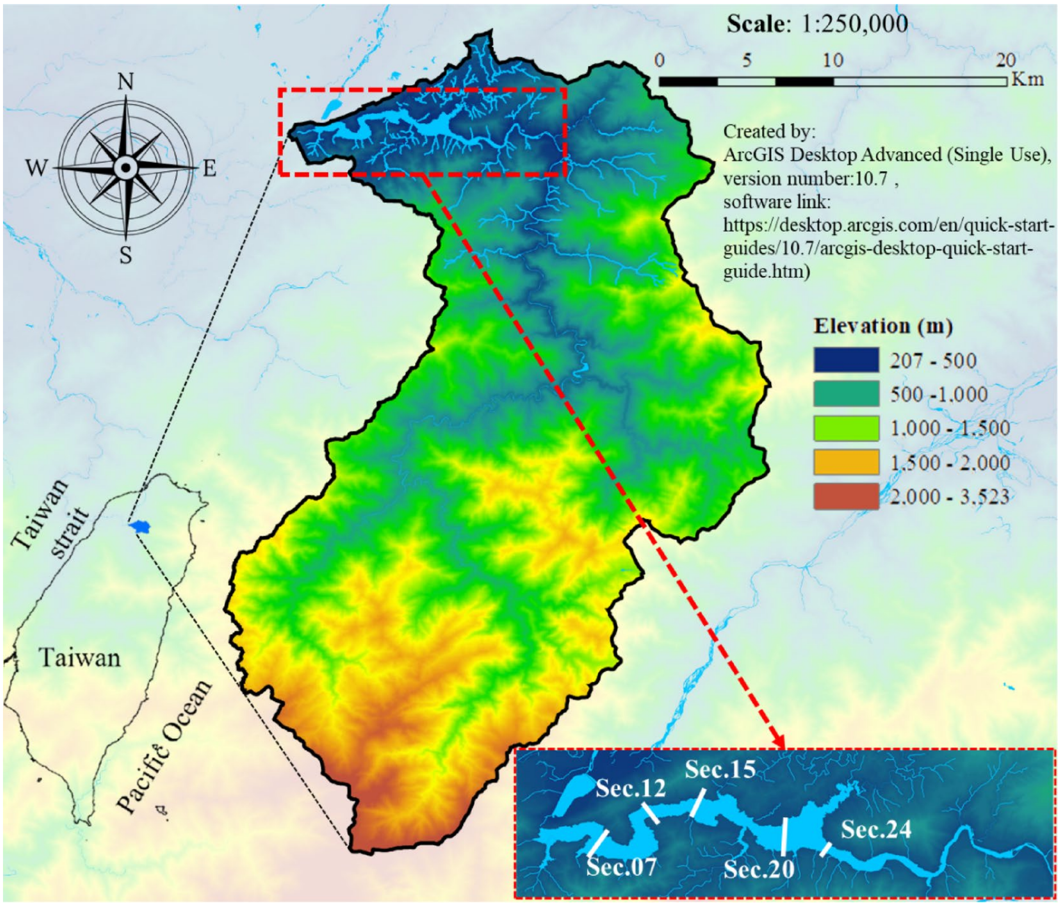

Fig. 1. Reservoir location and information (created by ArcGIS Desktop Advanced (Single Use), version number 10.7, https://desktop.arcgis.com/en/quick-start-guides/10.7/arcgis-desktop-quick-start-guide.htm).

instrument limitations. The relatively comprehensive data of three typhoon events, 2015 Typhoon Soudelor, 2015 Typhoon Dujuan, and 2016 Typhoon Megi were adopted to validate the simulation accuracy, and other typhoons can be the application case.

2015 Typhoon is ranked as the 1st huge inflow peak discharge, 5634 m^3/s, in the past decade, and the collected duration was 72 h. Typhoon Dujuan occurred after Soudelor; the peak discharge was 3802 m^3/s, and the measured duration was 62 h. The last historical event was the 2016 Typhoon Megi which lasted for 68 h, and the peak discharge was 4267 m^3/s. Besides, 2- to 200-year return-period cases are adopted to describe the slight, medium, severe, and extreme scenarios. The peak discharge (m^3/s) is 2251 for 2-yr, 4188 for 5-yr, 5327 for 10-yr, 6431 for 20-yr, 7855 for 50-yr, 8920 for 100-yr, and 9975 for 200-yr, respectively. The 2- and 5-yr cases represent the slight scenario; The 5-yr case, Dujuan and, Megi historical events represent the medium scenario; The serious typhoon in the past decade was 2015 Typhoon Soudelor; the peak discharge was between to 10- and 20-yr case, and these three represent the severe scenario; The most serious typhoon in the past fifty years was 2004 Typhoon Aere; the peak discharge was 8593 m^3/s, close to the 100-yr scenario. Typhoon Aere is difficult to be used in this research due to the lack of field data; fortunately, the 50- to 200-yr scenarios can be representative cases of the severe scenario. Finally, the 200-yr case can represent the extreme cases. The research cases list in Table 1.

Governing equation

Lai et al.[36] developed a 2D layer-averaged turbidity current model, SRH2D, which was later applied in a field reservoir by Hung. et al.[44]. The model uses the mass conservation and momentum equations to solve the hydraulic mechanism as shown in Eq. (1) to (3), as well as the non-equilibrium sediment transport equation uses to simulate turbidity current transportation as shown in Eq. (4) and (5). The initial and boundary condition is shown in the next chapter, and the specific description of numerical methods can be found in Lai et al.[36]

$$\frac{\partial h_t}{\partial t}+\frac{\partial h_t u_t}{\partial x}+\frac{\partial h_t v_t}{\partial y}=e_e U_t \tag{1}$$

$$\frac{\partial h_t u_t}{\partial t}+\frac{\partial h_t u_t u_t}{\partial x}+\frac{\partial h_t v_t u_t}{\partial y}=\frac{\partial h_t T_{txx}}{\partial x}+\frac{\partial h_t T_{txy}}{\partial y}-(RgC_t)h_t\frac{\partial Z_t}{\partial x}-\frac{Rg}{2}h_t^2\frac{\partial C_t}{\partial x}-(1+r_w)\frac{\tau_{xt}}{\rho_s} \tag{2}$$

$$\frac{\partial h_d v_d}{\partial t}+\frac{\partial h_d u_d v_d}{\partial x}+\frac{\partial h_d v_d v_d}{\partial y}=\frac{\partial hT_{txy}}{\partial x}+\frac{\partial hT_{tyy}}{\partial y}-(RgC_t)h_t\frac{\partial Z_t}{\partial y}-\frac{Rg}{2}h_t^2\frac{\partial C_t}{\partial y}-(1+r_w)\frac{\tau_{yt}}{\rho_s} \tag{3}$$

$$\frac{\partial h_t C_{kt}}{\partial t}+\frac{\partial h_t u_t C_{kt}}{\partial x}+\frac{\partial h_t v_t C_{kt}}{\partial y}=\upsilon_{kt}(p_{kt}E_{kt}-C_{bk}) \tag{4}$$

$$(1-\gamma_b)\frac{\partial Z_{bt}}{\partial t}=-\sum_k \upsilon_{kt}(p_{kt}E_{kt}-C_{bk}) \tag{5}$$

where, h_t: turbidity current thickness; t: time; x and y: x- and y-direction in Cartesian coordinates; u_t and v_t : velocity in the x- and y-directions; U_t: average velocity defined as $\sqrt{u^2+v^2}$; e_e: dimensionless entrainment coefficient; $T_{txx}, T_{txy}, T_{tyy}$: dispersion terms; R: submerged specific gravity of sediment in the turbidity current (=ρ_D/ρ_w-1); ρ_D: density of sediment; ρ_w: density of ambient water; g: acceleration of gravity; C_t: total suspended sediment concentration; Z_t: current top elevation; r_w: friction between upper ambient water and the bottom turbidity current; ρ_s: mixture density; τ_{xt} and τ_{yt}: bed shear stresses in x- and y- direction; C_{kt}: near-bed concentration of the k_{th} size class; υ_{kt}: fall velocity of the k_{th} sediment size class; p_{kt}: volume fraction of the k_{th} sediment size class; E_{kt}: erosion rate potential; C_{bk}: near-bed concentration of the k_{th} size class; γ_b: porosity of bed sediment; Z_{bt}: bed elevation.

Initial and boundary condition

The calibrated parameter setting is essential to ensure the simulation accuracy in the field site. This article adopted the part of the setting from Huang et al.[40] and Hung et al.[44] to set the simulation parameters. The turbulence model adapts to the parabolic model; The gravity of sediment is 2700 (kg/m^3). Based on Huang et al.[40], the drag

Type	Case	Peak discharge (m^3/s)	validate	Application	
Historical event	Soudelor	5634	o	o	Severe
	Dujuan	3802	o	o	Medium
	Megi	4267	o	o	Medium
Return-period	2-yr	2251		o	Slight
	5-yr	4188		o	Medium
	10-yr	5327		o	Severe
	20-yr	6431		o	Severe
	50-yr	7855		o	Extreme
	100-yr	8920		o	Extreme
	200-yr	9975		o	Extreme

Table 1. Research cases list.

coefficient was calibrated using field data and references like Huang et al.[40], with 0.002 found optimal. The time step (0.5–1.0 s) balances computational efficiency and accuracy, avoiding numerical instability. Grid numbers ranged from 4000 to 20,000; 10,230 were chosen for optimal spatial resolution and computational feasibility. In addition, the model calibration took approximately 5 h for a historical typhoon case. The proportion of CPU and real-time is close to 1–10, which means the numerical model needs an hour to simulate 10 h in field time.

The simulation grid, elevation, and essential information are shown in Fig. 2.

In order to develop a practical prediction approach in the field site, this study gathered three relatively complete time-series field data, including the inflow and outflow hydrology and sediment data. Additionally, different return-period scenarios were also added to represent the slight, medium, severe, and extreme disaster scale to validate the consistency of the simulation model in different scenarios. The description of the adapted cases shows in "Chapter 2.2".

Research framework

This study presents the most convenient and cost-effective three-stage approach for managing reservoir water resources based on understanding the turbidity current in temporal and spatial variation. It not only focuses on the satisfactory prediction result of turbidity current movement but also formulates an appropriate sluice gate operation approach to take care of reservoir desiltation and water resources conservation during flood duration based on the guideline rule and value presented in this research. The research flowchart is shown in Fig. 3.

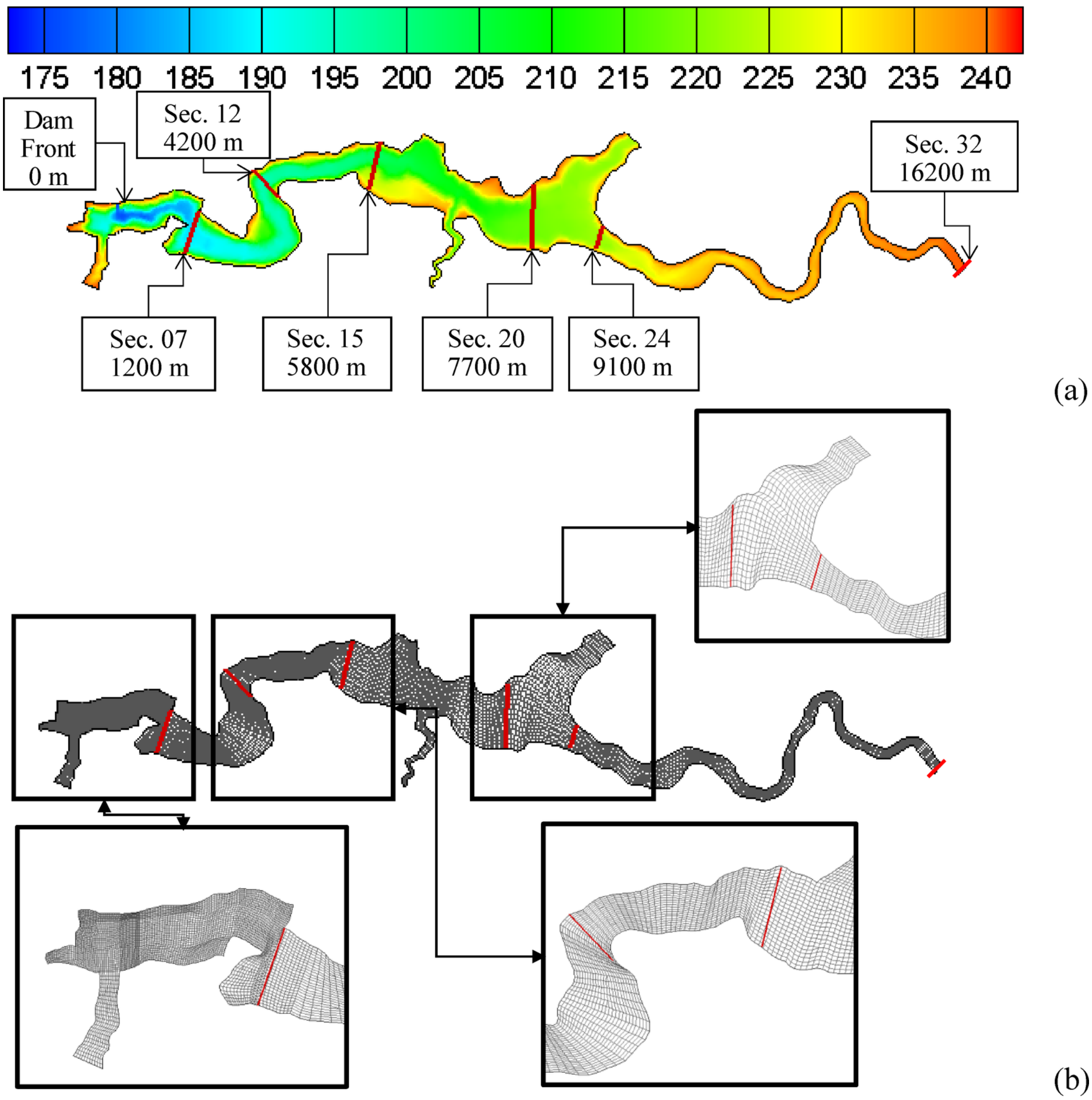

Fig. 2. Simulation (**a**) elevation; (**b**) grids.

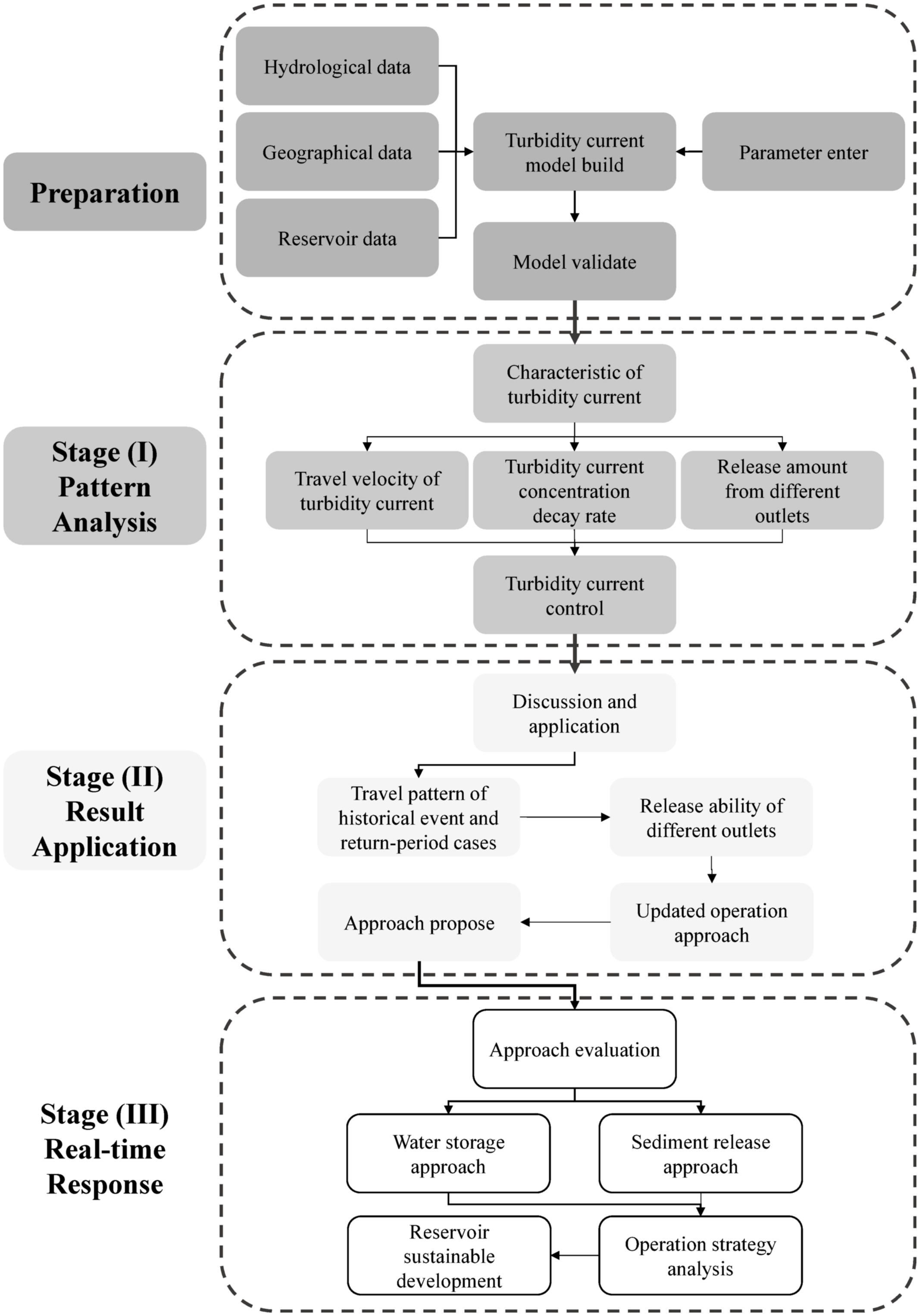

Fig. 3. Research flowchart.

Result

Travel velocity

The movement of the turbidity current is non-conservative due to the interaction of gravity and buoyancy. The channel shape, such as construction, expansion, or flexural all affect the energy loss to change the travel pattern[45,46]. Besides, the inflow conditions are the crucial factors that affect the turbidity current. National Chiao Tung University[47] figure out that the discharge, concentration, and hydrograph period are highly-related to the generation timing of turbidity current: (i) inflow peak discharge > 1800 m^3/s; (ii) inflow peak concentration > 15,000 mg/L; (iii) inflow duration lasted more than 35 h of 350 m^3/s. Therefore, three typhoons satisfied with the above criteria are adopted to validate the travel velocity along the reservoir.

Reservoir management requires an accurate estimation of the travel velocity of a turbidity current, as the appropriate timing for hydraulic desilting depends on it. In other words, the robust simulation of the travel velocity along the reservoir can use to predict the turbidity current movement and formulate the sediment release strategy early. Figure 4 compares the travel velocity of three typhoons between measurement and simulation. S24, S20, S15, S12, and S07 are located at 9100 m, 7700 m, 5800 m, 4200 m, and 1200 m, respectively, and were adopted to evaluate the accuracy between measurement and simulation. The relatively slow velocity shown in S24 to S20 in typhoon Soudelor and Megi because the cross-section is larger than the other location, and the value is 0.39 and 0.33 in Typhoon Soudelor; 0.26 and 0.21 in Typhoon Megi between measured and simulated data, respectively. In addition, the data from S20 of Typhoon Dujuan were missing and challenging to compare. Then, the gradually speed-up trend is presented in S24 to S15, S24 to S12, and S24 to S12 both measurement and simulation. The measured and simulated value of Soudelor, Dujuan, and Megi is 0.23 and 0.19; 0.14 and 0.14; 0.18 and 0.15, from S24 to S15. Besides, the value from S24 to S12 is 0.25 and 0.23; 0.18 and 0.18; 0.23 and0.19. And 0.29 and 0.28; 0.27 and 0.26; 0.29 and 0.26 (S24–S7). Note that, the coefficient of determination also presents in Fig. 3, and the highly positive correlation trends is indicated by the R^2 value, 0.92.

The above content shows the simulation accuracy of travel velocity; namely, the temporal-spatial variation of turbidity current along the reservoir can be estimated by using this model. Next, the variation of turbidity current concentration needs to be validated to understand the applicability in the field site further.

Concentration variation

This chapter describes a study on the sediment transport distance in the Shihmen Reservoir during different typhoons to determine the variation of the sediment concentration with distance. The unit concentration decay rate of the density current is presented to avoid the affecting of different cross-section widths. The comparison of the measurement and simulation of the unit concentration decay rate at different cross-sections (S32, S24, S20, S15, S12, and S07) along the reservoir shows in Fig. 5 and described below.

Firstly, the simulated result shows an accurate decay rate from S32 to S07. The decay value of the measured and simulated result is 0.09 and 0.08 in Typhoon Soudelor; 0.08 and 0.08 in Typhoon Dujuan; 0.08 and 0.08 in Typhoon Megi. In other words, the unit concentration decay rate is usually less than 0.1 from the entrance to the dam front and the simulation can obtain accurate values in different typhoons. Then, the simulated values from S32 to S24 to S15 to S7 are 0.52 to 0.11 to 0.08 in Typhoon Soudelor; 0.51 to 0.12 to 0.08 in Typhoon Dujuan; 0.46 to 0.12 to 0.08 in Typhoon Megi, and the corresponding measured; the values are 0.67 to 0.06 to 0.09 in Typhoon Soudelor; 0.62 to 0.06 to 0.08 in Typhoon Dujuan; 0.23 to 0.06 to 0.08 in Typhoon Megi. Compared to the simulation and measurement, the decay rate, the simulated decay value shows a consistent decreasing trend in three typhoons along the reservoir. In contrast, the measured data shows decreasing trends from S32 to S15 and increasing trends from S15 to S7, and it is unreasonable because the sediment source between S15 to S07 is zero. In addition, the decay value, 0.23, from S32 to s24 shown in Typhoon Megi is outlier, because

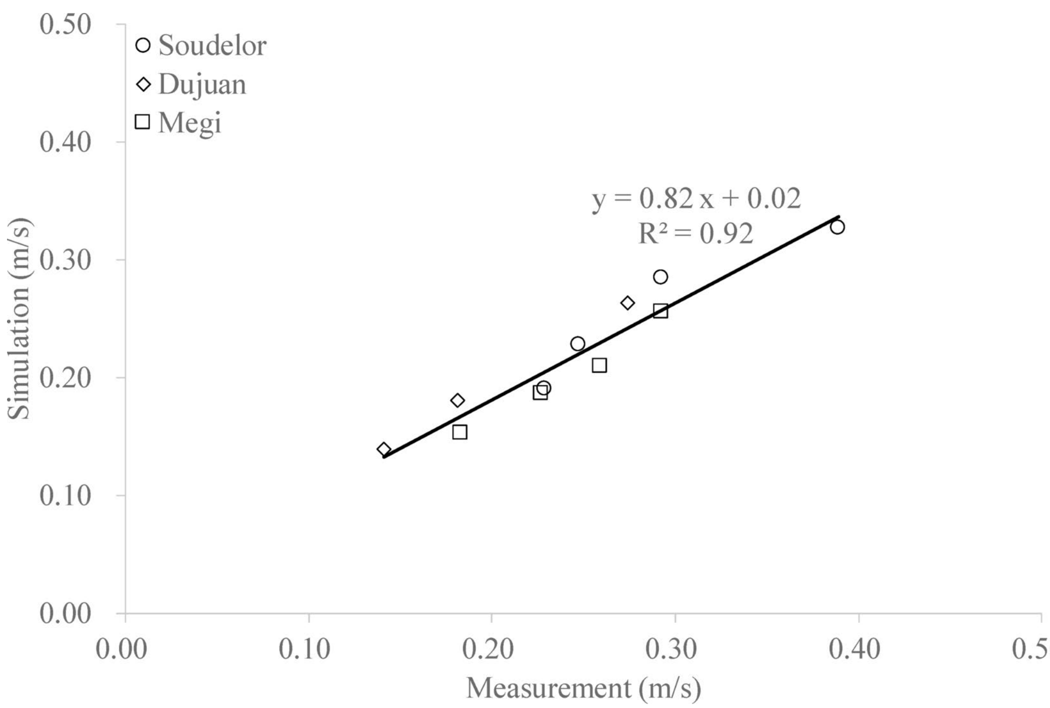

Fig. 4. Comparison of travel velocity between measurement and simulation.

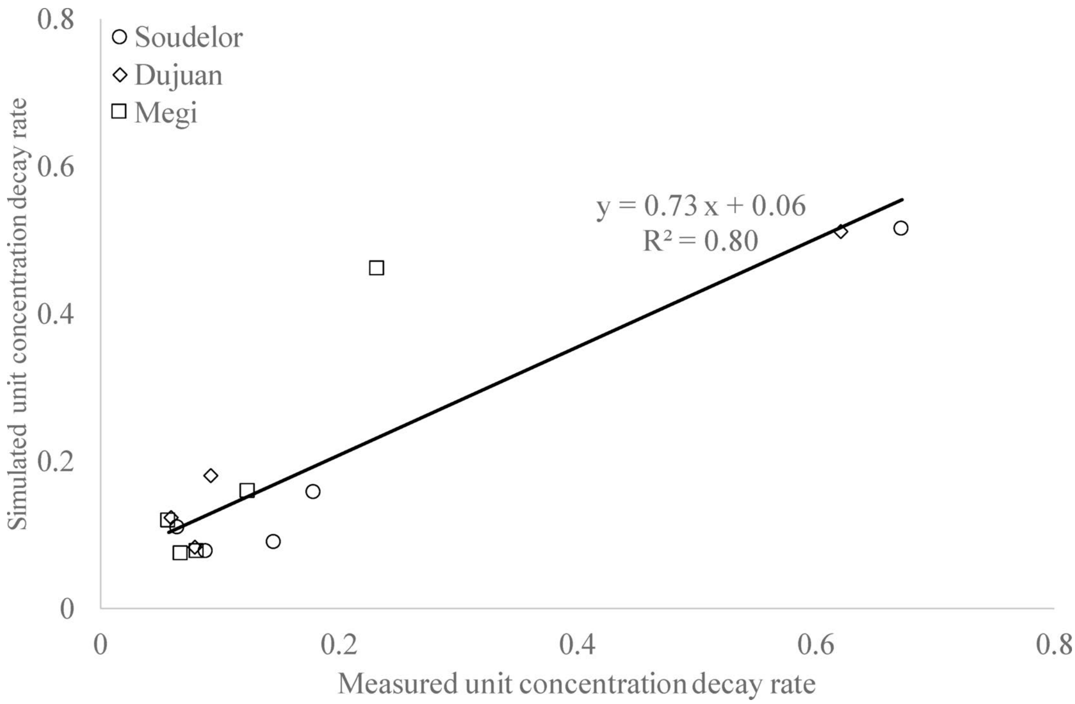

Fig. 5. Comparison of travel velocity between measurement and simulation.

the measured values in Typhoon Soudelor and Dujuan are 0.67 and 0.62. The most important is that the highly positive correlation trend is still presented by considering all measured and simulated data, the R^2 value is 0.80.

The above description indicates that the simulated sediment concentration shows a close decay rate by comparing it with the measurement. Note that the simulation can effectively grasp the sediment concentration variation along the reservoir, especially near the dam front. Finally, the simulated release amount from different outlets during different typhoons will be presented to compare with the measured release to validate the practical in the next chapter.

Release amount

The release amount during typhoons is a crucial factor in dealing with reservoir deposition issues. The release ability of different outlets needs to be investigated to formulate a suitable desilting strategy. Below is a comparison of measurement and simulation release amounts.

Figure 6 presents the release amount of Spillway Fig. 5 presents the total release amount from Spillway, Shihmen Canal, and Bottom Outlet located at the dam front in three typhoons. Each release amount (m^3) of simulation and measurement in Typhoon Soudelor are 62,881 and 71,071 from Spillway; 4732 and 4459 from Shihmen Canal; 135,226 and 143,689 from Bottom Outlet. In addition, the total release amount (m^3) of measurement and simulation in Typhoon Soudelor is 202,839 and 21,9219, and the total inflow amount is 910,000. The above information indicates that the simulation can reflect the actual release amount because the difference between simulation and measurement is just 0.90%, 0.93%, and 0.03% in Spillway, Shihmen Canal, and Bottom Outlet. The release data the other two typhoons are shown below: 30,291 and 25,047 from Spillway; 3381 and 4071 from Shihmen Canal; 62,514 and 119,370 from Bottom Outlet in Typhoon Dujuan. 58,110 and 70,590 from Spillway; 3770 and 3380 from Shihmen Canal; 110,630 and 80,470 m^3 from Bottom Outlet in Typhoon Megi. This study adopts those data to regress to understand the relative correlation between the simulation and measurement. The regression curve shows a highly related trend, $R^2 = 0.81$.

The comparison of release amount indicates that the numerical model has sufficient simulation performance in different sluice gates, especially for the Spillway Shihmen Canal. It means that the simulation can reasonably estimate the release information and is more consistent than the measurement because the measured instrument sometimes misses data due to environmental issues and measured limitations. Overall, based on the simulated turbidity current flow, including travel velocity, concentration decay rate, and release amount, the simulation method can be a practical forecasting tool for reservoir desilitation. The specific discussion is shown in "4. Discussion".

Discussion

This study aims to grasp the turbidity current movement and provide a more efficient sediment release operation during typhoons. Note that the turbidity current's travel pattern along the reservoir provides a well-described sedimentation mechanism. To compare to the original operation, an updated reservoir operation approach is proposed for different goals, such as deposited removal, water storage, etc. Please see the following description.

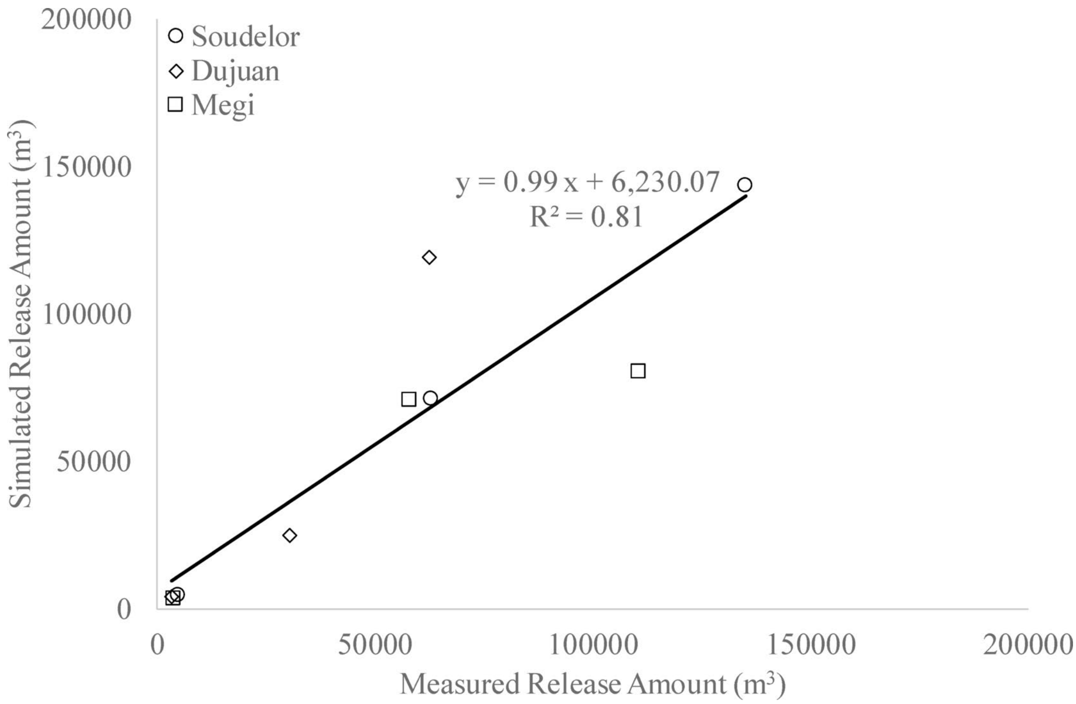

Fig. 6. Comparison of release amount between measurement and simulation.

Relationship of turbidity current discharge, velocity, and unit concentration

This study investigated the travel velocity between different cross-sections along the reservoir and obtained an accurate result in Chapter 3. The simulated cases were from three typhoon events, namely Typhoon Soudelor, Dujuan, and Megi. This chapter studies the relationship between peak discharge and travel velocity of the turbidity current flow and figures out a robust outcome that presents a positive correlation. The highest peak discharge, 5634 m^3/s, was observed during Typhoon Soudelor, while the middle value, 4267 m^3/s, was seen during Typhoon Megi, and the event with the lowest peak discharge was Typhoon Dujuan which is 3802 m^3/s. Results indicate that the travel velocity is directly proportional to the peak discharge, as evidenced by Soudelor, 0.45 m/s, and Megi, 0.43 m/s, and the travel velocity of Dujuan ranked third, at 0.42 m/s. Furthermore, Different return-period cases were imported such as 2- (2251 m^3/s), 5- (4188 m^3/s), 10- (5327 m^3/s), 20- (6431 m^3/s), 50- (7855 m^3/s), 100- (8920 m^3/s), and 200-year scenario (9975 m^3/s) to extend the estimated range of the travel velocity. The results show that the peak discharge and travel velocity also increase as the return period increases. For example, the 200-year return period case has the highest peak discharge and travel velocity, which further supports the positive correlation between peak discharge and travel velocity. Besides, this research adopts simulation of historical events, different return-period cases, and measurement of three typhoons to establish the regression relationship. The linear regression curve indicates that the peak discharge and travel velocity have a highly positive relative, $R^2 = 0.86$. The above explanations show in Fig. 7 the relationship between Dimensionless discharge (DQ = Q/QMax) and Dimensionless velocity (DV = V/VMax), where QMax and VMax represent the discharge and velocity of the 200-year scenario.

Updated operation approach for desiltation

Due to the dam safety issue, the current reservoir operation guideline relies on the variation in water level to release the inflow discharge. However, understanding the sedimentation mechanism to determine a suitable strategy for reservoir deposition is also crucial in maintaining dam construction. Finding the balance between discharge and sediment release is the essential purpose of this paper. Reservoir management heavily relies on accurately determining the travel velocity of density currents, which is crucial in determining the appropriate timing for hydraulic desilting. An accurate travel velocity improves sediment release efficiency and helps conserve water resources.

This research compares the three significant typhoons during 2015 and 2016, which have collected relatively complete data. A consistent operation principle is presented that the spillway was responsible for the primary release work because the design discharge is the largest to fast response the enormous inflow of material. The percentage of the spillway, spillway tunnel, shihmen canal, power generation intake, modification tunnel, and permanent river outlet are 57.95, 21.68, 1.62, 7.43, 7.16, and 4.16, respectively. Besides, the percentage of the spillway and other outlets is 39.49 and 60.51 in Typhoon Dujuan and 48.01 and 51.99 in Typhoon Megi. That means at least 40% of inflow material was released from the spillway during these three typhoons. In contrast, the percentage of released sediment from the spillway was 10.37, 3.87, and 6.67%, respectively, in Typhoon Soudelor, Dujuan, and Megi; 25.90, 33.46, and 13.25% released from the other outlets. The analysis of the ratio

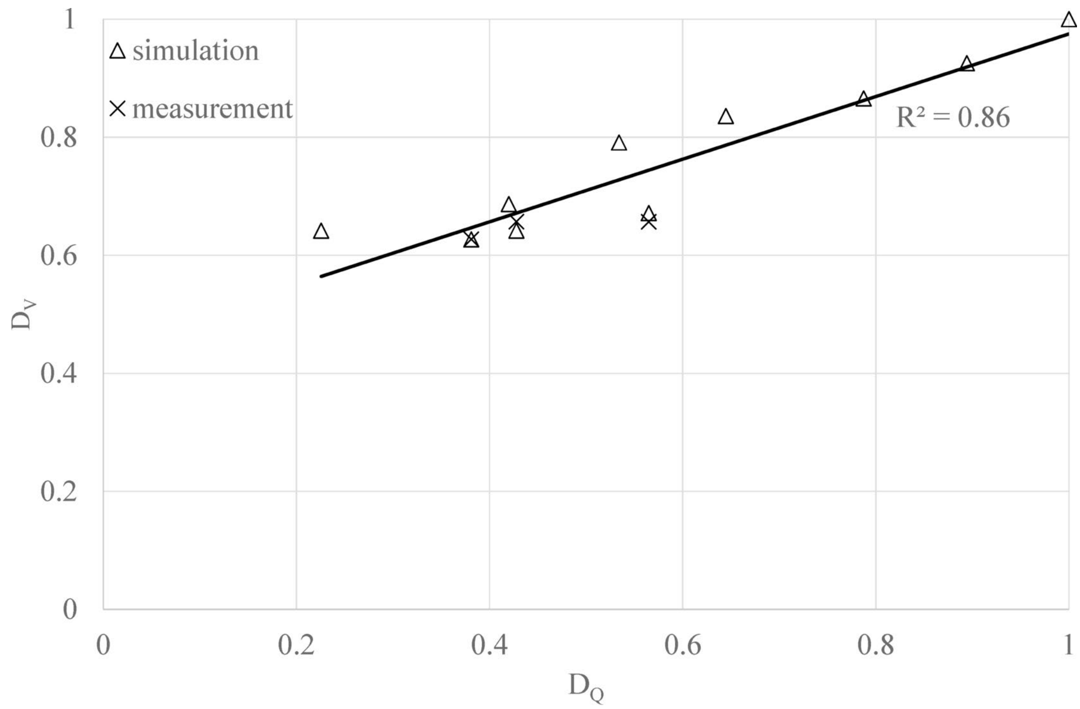

Fig. 7. Relationship between DQ and DV.

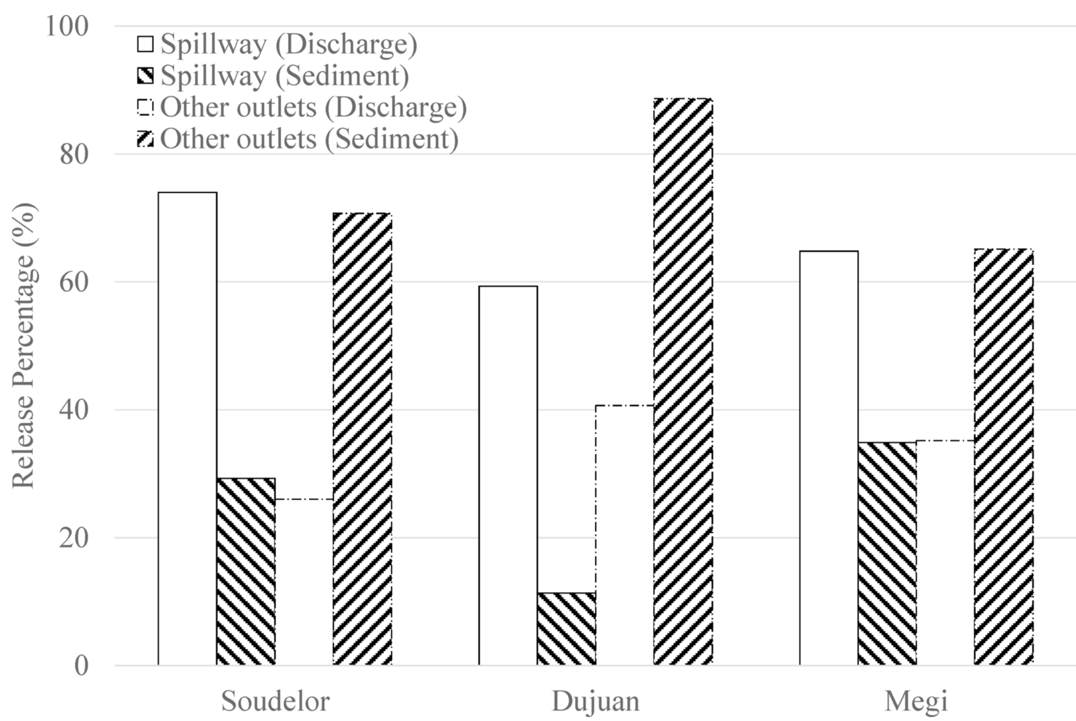

Fig. 8. Release percentage of three historical typhoon events.

of the release discharge and sediment is shown in Fig. 8. Above all, the release ability of the spillway presented a lower efficiency and the operation process can be updated to increase the sediment release amount.

A critical concern, and the primary principle of reservoir operation during typhoon periods should be to release more sediment. Technically speaking, reservoir water level significantly influences sediment release efficiency. However, in Taiwan, most reservoirs serve as crucial water supply sources. The priority is given to balancing flood control, sediment management, and water supply rather than actively lowering the water level for sediment flushing during typhoon events. Above all, the modification operation procedure could be the feasible strategy. Based on historical records, the inadequacy of sediment release through the spillway is evident in the three different typhoons depicted in Fig. 8. Using a relatively lower outlet to release the inflow of sediment is worthwhile. The modification tunnel could be a suitable solution as it has a discharge capacity of 300 m^3/s, the highest release discharge of all bottom outlets.

Two modified operation methods based on actual operations were implemented and presented in Fig. 9. The scenario (I) addresses water resource management and reservoir desiltation. It involves redirecting the release discharge from the spillway to the modification tunnel, with a time shift of 9 h applied to align with the arrival timing of turbidity currents along the time series. This modification aims to optimize sediment release while considering the preservation of water resources. The scenario (II) focuses primarily on reservoir desiltation. In this case, the modification tunnel operates continuously throughout the entire duration of the typhoon event after turbidity current flow arrival, aiming to maximize sediment discharge and maintain the reservoir storage capacity. The comparison between Scenario 1, Scenario 2, and Actual operation is based on the 2015 Typhoon Soudelor event, which had the highest peak discharge (5634 m^3/s) among the historical events analyzed in this study. This selection ensures that the operational strategies are evaluated under extreme hydrological conditions, providing valuable insights into the effectiveness of different sediment release approaches.

Figure 10 indicates that the modified operation strategies present a better sediment-released ability. Firstly, actual operation and scenario (I) are selected to compare the release efficiency of all sluice gates. Except for the spillway and the modification tunnel, the other four outlets show the close value because the operation keeps the same between the actual and scenario (I). The sediment-released amount of the spillway presents more than two times the actual operation, from 67,619 to 153,107 m^3. The primary factor is the operation time delay of nine hours. The release amount is challenging for sufficiency efficiency until the turbidity current arrives at the dam front. The time-shifting operation improves the sediment-released efficiency and maintains the water resources. In addition, the modification tunnel also shows high release efficiency from 53,846 to 128,071 m^3. Secondly, this study adapts scenarios (I) and (II) to analyze the sediment-released number of different outlets. The modification tunnel plays a significant role in releasing the reservoir sediment, and the sediment-released amount reached 294,283 m^3 during the typhoon period. Although the released sediment from the power generation intake and permanent river outlet decreased from 69,077 to 61,340, from 76,457 to 64,646 m^3, respectively, the total release amount is higher than the scenario (I). The crucial factor is the long-term operation of the modification tunnel in this typhoon to raise the release amount from 128,071 to 294,283 m^3. Most importantly, scenarios (I) and (II) present a release amount that is sufficient for the actual operation. The total release amount is 309,752, 474,533, and 621,204 m^3 of actual (I) and (II). As a result, a good grasp of turbidity current flow is a critical issue because it can help reservoir management reorganize the release strategy further to improve the release efficiency of the reservoir sediment. Table 2 presents a comparative analysis of sediment release efficiency under different operational scenarios. The data highlight the impact of varying discharge conditions on turbidity current behavior and sediment transport efficiency. By comparing the actual operation with the two modeled scenarios, the results demonstrate that optimized sediment release strategies can significantly enhance desiltation efficiency. The findings underscore the importance of adaptive reservoir management in responding

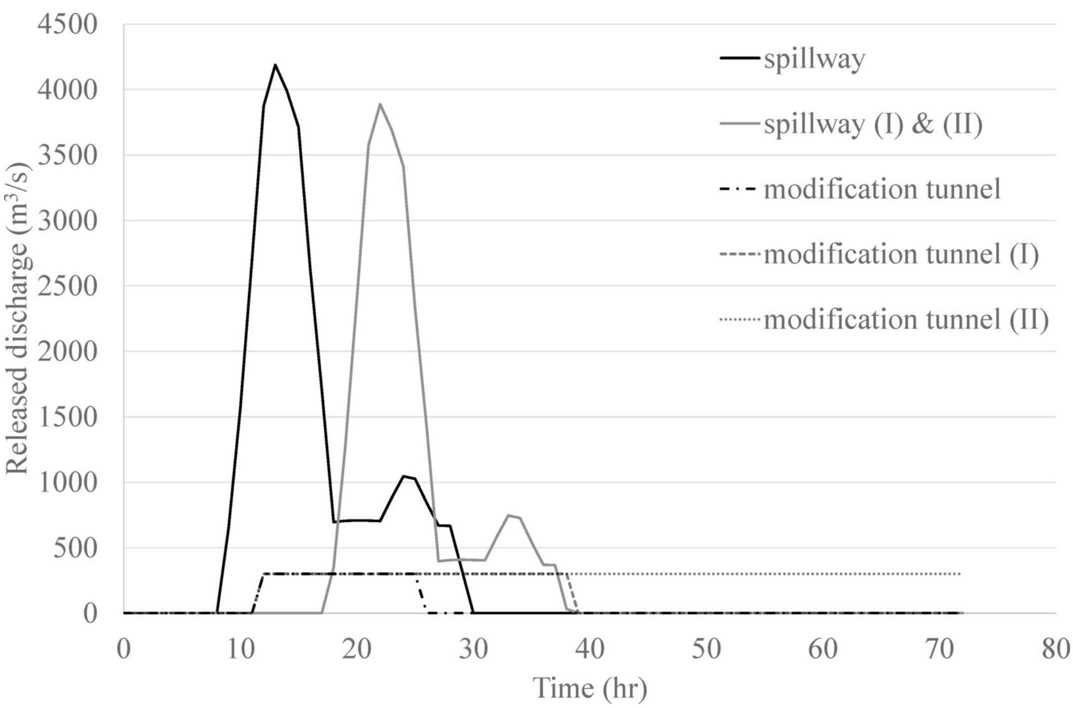

Fig. 9. Modified operation of spillway and modification tunnel.

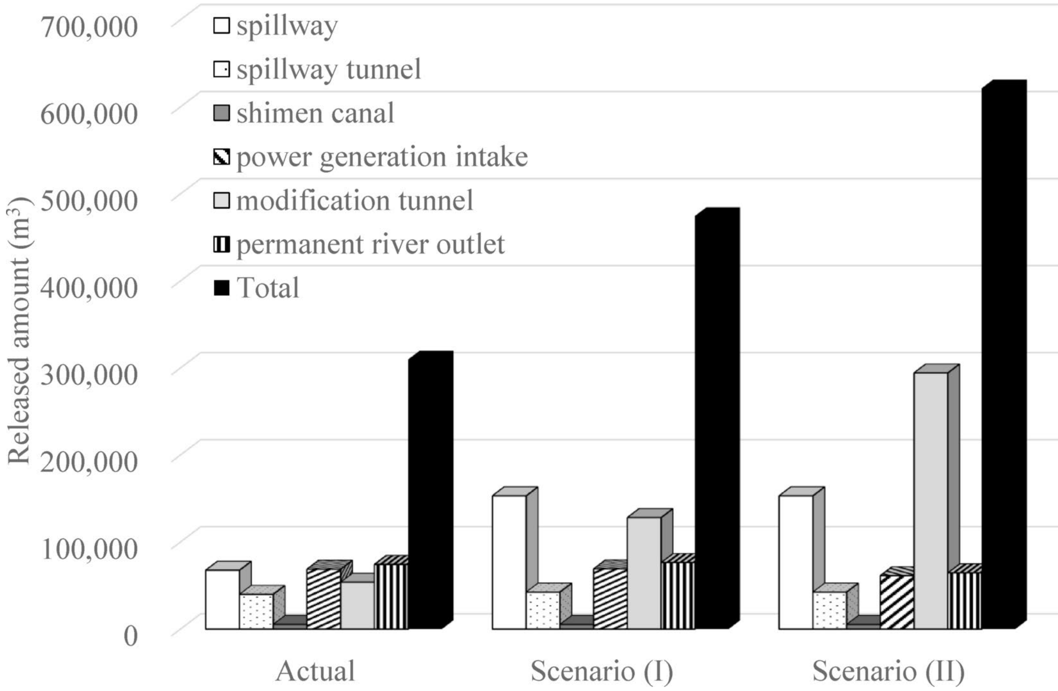

Fig. 10. Updated released amount of different operation strategies.

Case	Release water (1)	Release sediment (2)	Proportion [(1)/(2)] = (3)
Actual	1	1	1
Scenario (I)	0.96	1.52	1.58
Scenario (II)	1.13	2.00	1.77

Table 2. Research cases list. *Actual (1), (2), (3) means the baseline.

to fluctuating hydrological conditions, ensuring a balance between sediment flushing and water storage. This comparison provides valuable insights for improving reservoir sediment control strategies, supporting more effective decision-making in water resource management.

Updated operation approach for water conservation

Most of the water sources are from typhoons and flood events, and the proper real-time approach needs to be formulated to respond to the sluice gate operation timing. The strategy for sediment release from a reservoir can be divided into two conditions: flood control operation condition and non-flood control operation condition. The efficiency of sediment release during the flood control operation period can be improved as described in Sect. "Updated operation approach for desiltation". Sediment release operation after the arrival of high-density flow can achieve the best desilting efficiency. For the sediment release strategy during the non-flood control operation condition, consideration should be given to whether the reservoir storage capacity meets the water resource supply. When the water resource supply is sufficient, that is, the storage capacity of the reservoir is greater than the upper limit of the reservoir operating rule, the cost of water resource utilization should be taken into account.

The main desilting strategy for the dredging at the front of the Shihmen Reservoir in Taiwan is mechanical dredging, with a dredging cost of about \$17 USD/m^3[44]. Based on the background conditions of the dry density of sediment of about 735 kg/m^3[48] and a public water supply fee of about \$ 0.36 USD per ton of public water supply, if hydraulic sediment desilting is used as an alternative to mechanical dredging at the same cost, the required water volume for hydraulic sediment desilting can be calculated based on the same cost of public water supply. When the sediment concentration reaches about 11,717 mg/L and it can be estimated by the presented numerical model, the same opportunity cost can be achieved. Therefore, this principle can be used as the basis for the sediment release operation of the target reservoir during the non-flood control operation condition.

$$S_f = \frac{S_w \times 10^3}{(S_w/S_d) + [D_c/P_c/(1 - S_w/S_d]} \quad (6)$$

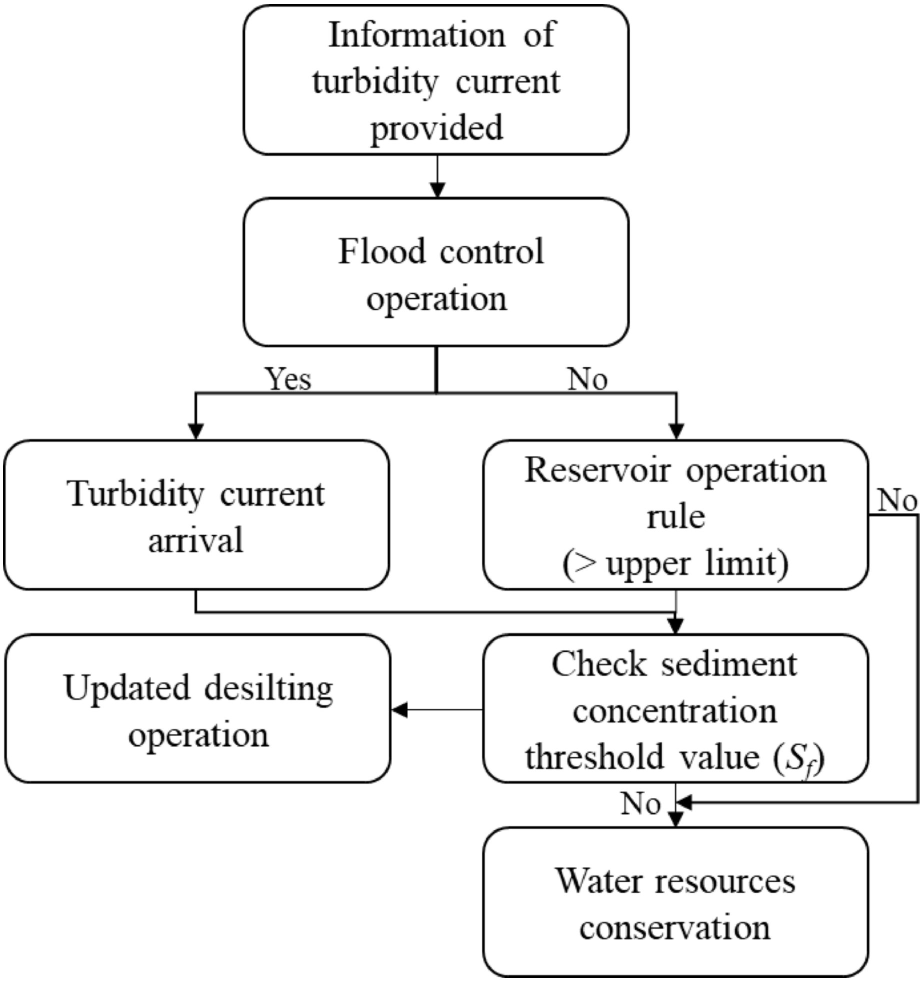

Fig. 11. Real-time response procedure in different scenarios during a typhoon event.

where, S_f: sediment concentration threshold value (mg/L); S_w: sediment weight (kg = dry density (kg/m) of deposited sediment $\times 1m^3$); S_d: sediment density (kg/m^3) ; D_c: Dredging cost ($) ;$P_c$: Public water supply cost ($).

Real-time response system

The crucial point of the reservoir operation during typhoon periods is a sufficient response time to organize the relative strategy. Hence, a useful real-time response system established by the numerical model needs to consider the computing efficiency of the actual typhoon. This research used a personal computer (PC) to conduct the computing time test. The specification of the central processing unit (CPU) is 12th Gen Intel(R), Core (TM) i7-12700, 2.10 GHz; the random-access memory is 32.0 GB. The adopted typhoon duration is 3 days, 72 h, and the total computing time is 0.96 h. In other words, the current specification of the PC only needs 48.06 s to provide relative information on reservoir turbidity current flow after 1-h. Furthermore, the turbidity current flow is proven to need more than 1 h to transport to the dam front. It means the proposed real-time response system can obtain sufficient time to formulate the operation procedure.

The analysis of the primary sediment release operation strategy for the reservoir can be referred to in Fig. 11. Providing robust information on the turbidity current flow is essential, then the flood control operation could be formulated in two situations. Here, "Yes" means the reservoir needs to release the inflow material to protect the safety of the dam. The dynamic state of the turbidity current provides an immediate estimate of the operation timing from different outlets. The threshold value is the second parameter to determine operation duration to maximize the sediment-releasing amount. The effectiveness of the updated desilting operation is shown in Chapter 4.2. 'No' means the inflow discharge is not a threat, and water resources need to be conserved in the current period. Hence, the time-series sediment concentration has to be monitored and compared to the threshold value. If the value is lower than the upper limit, the reservoir can store the water resources. In contrast, the desilting operation should be conducted to avoid sediment depositing on the reservoir bed to decrease the storage capacity. The proposed real-time approach for reservoir storage and desiltation operation is a rolling update method. It is practical to prolong the reservoir operation lifespan and conserve sufficient water resources after typhoons.

Conclusion

This study aims to provide an accurate approach for predicting turbidity current flow to understand sediment transport dynamics better. It also proposes enhancements to sediment release efficiency at the major outlet structures near the dam front. To achieve this, a three-stage research procedure is presented, which includes flow pattern analysis, updated operational strategies, and economic evaluation. This procedure forms a robust foundation for sustainable reservoir operation and water resource planning.

The structured three-stage framework is a basis for optimizing sediment release operations during non-flood control periods. A real-time response procedure tailored to various typhoon scenarios is implemented for flood events. The proposed rolling-update method enhances reservoir storage and sediment flushing operations, extending reservoir functionality and improving post-typhoon water conservation.

This study offers valuable insights into the temporal and spatial variations of sediment transport in Shihmen Reservoir during typhoon events. The findings support better management of sediment deposition, which significantly impacts both storage capacity and economic performance. The proposed approach optimizes sediment release strategies, improving flood control and water conservation. Furthermore, the core concept of real-time numerical prediction can serve as a foundation for future field applications and research.

Data availability

Data is provided within the manuscript.

Received: 2 January 2025; Accepted: 21 April 2025
Published online: 29 April 2025

References

1. Samad, N. et al. Sediment yield assessment and identification of check dam sites for Rawal Dam catchment. *Arab. J. Geosci.* **9**(6), 6. https://doi.org/10.1007/s12517-016-2484-9 (2016).
2. Zeng, Y. et al. Estimation of the volume of sediment deposited behind check dams based on UAV remote sensing. *J. Hydrol.* **612**, 128143. https://doi.org/10.1016/j.jhydrol.2022.128143 (2022).
3. Zulfan, J., Ginting, B. M., & Rimawan, R. Assessment of reservoir sedimentation and mitigation measures using 2D hydrodynamic modeling: Case study of Pandanduri Reservoir, Indonesia. In *IOP Conference Series: Earth and Environmental Science* vol. *1135*(1), Article 1 (2023). https://doi.org/10.1088/1755-1315/1135/1/012018
4. Ge, H., Zhu, L., Lin, Q. & Deng, C. Analysis of sediment deposition in Lushui Reservoir to guide dredging. *Arab. J. Geosci.* **14**(2), 2. https://doi.org/10.1007/s12517-021-06512-w (2021).
5. Kantoush, S. A., Mousa, A., Shahmirzadi, E. M., Toshiyuki, T. & Sumi, T. Pilot field implementation of suction dredging for sustainable sediment management of dam reservoirs. *J. Hydraul. Eng.* **147**(2), 2. https://doi.org/10.1061/(ASCE)HY.1943-7900.0001843 (2021).
6. Smith, C., Williams, J., Nejadhashemi, A. P., Woznicki, S. & Leatherman, J. Cropland management versus dredging: An economic analysis of reservoir sediment management. *Lake Reserv. Manag.* **29**(3), 3. https://doi.org/10.1080/10402381.2013.814184 (2013).
7. Albayrak, I., Müller-Hagmann, M., & Boes, R. Efficiency evaluation of Swiss sediment bypass tunnels. In *Proceedings of the 3rd International Workshop on Sediment Bypass Tunnels* 239–245 (2019). https://doi.org/10.3929/ethz-b-000337945
8. Boes, R., Müller-Hagmann, M. & Albayrak, I. Design, operation and morphological effects of bypass tunnels as a sediment routing technique. In *Proceedings of the 3rd International Workshop on Sediment Bypass Tunnels* 40–50 (2019). https://doi.org/10.3929/ethz-b-000337946
9. Morris, G. L. Classification of management alternatives to combat reservoir sedimentation. *Water* **12**(3), 3. https://doi.org/10.3390/w12030861 (2020).
10. Annandale, G. W., Morris, G. L. & Karki, P. *Extending the life of reservoirs* (World Bank, 2016).
11. Obialor, C. A., Okeke, O. C., Onunkwo, A. A., Fagorite, V. I. & Ehujuo, N. N. Reservoir sedimentation: Causes, effects and mitigation. *Int. J. Adv. Acad. Res.* **5**(10), 10 (2019).
12. Boulange, J., Hanasaki, N., Yamazaki, D. & Pokhrel, Y. Role of dams in reducing global flood exposure under climate change. *Nat. Commun.* **12**(1), 1. https://doi.org/10.1038/s41467-020-20704-0 (2021).
13. Chong, K. L., Lai, S. H., Ahmed, A. N., Wan Jaafar, W. Z. & El-Shafie, A. Optimization of hydropower reservoir operation based on hedging policy using Jaya algorithm. *Appl. Soft Comput.* **106**, 107325. https://doi.org/10.1016/j.asoc.2021.107325 (2021).
14. Gorguner, M. & Kavvas, M. L. Modeling impacts of future climate change on reservoir storages and irrigation water demands in a Mediterranean basin. *Sci. Total Environ.* **748**, 141246. https://doi.org/10.1016/j.scitotenv.2020.141246 (2020).
15. Huang, C.-C., Lai, J.-S., Lee, F.-Z. & Tan, Y.-C. Physical model-based investigation of reservoir sedimentation processes. *Water* **10**(4), 4. https://doi.org/10.3390/w10040352 (2018).
16. Lee, F.-Z., Lai, J.-S. & Sumi, T. Reservoir sediment management and downstream river impacts for sustainable water resources—Case study of Shihmen reservoir. *Water* **14**(3), 3. https://doi.org/10.3390/w14030479 (2022).
17. Turner, S. W. D., Steyaert, J. C., Condon, L. & Voisin, N. Water storage and release policies for all large reservoirs of conterminous United States. *J. Hydrol.* **603**, 126843. https://doi.org/10.1016/j.jhydrol.2021.126843 (2021).
18. Ghorbanzadeh, O., Crivellari, A., Ghamisi, P., Shahabi, H. & Blaschke, T. A comprehensive transferability evaluation of U-Net and ResU-Net for landslide detection from Sentinel-2 data (case study areas from Taiwan, China, and Japan). *Sci. Rep.* **11**(1), 1–20 (2021).
19. Nazir, M. H. M. et al. Sediment transport dynamic in a meandering fluvial system: Case study of Chini River. In *IOP Conference Series: Materials Science and Engineering* vol. 136, no. 1 012072 (2016). https://doi.org/10.1088/1757-899X/136/1/012072
20. Akbarizadeh, M., Saffarian, M. R. & Ghomeshi, M. Experimental investigation of sediment accumulation reduction in reservoirs due to turbidity currents with channel insertion at the entrance. *Int. J. Civ. Eng.* **18**(1), 1. https://doi.org/10.1007/s40999-019-00458-7 (2020).
21. Cesare, G. D., Schleiss, A. & Hermann, F. Impact of turbidity currents on reservoir sedimentation. *J. Hydraul. Eng.* **127**(1), 1. https://doi.org/10.1061/(ASCE)0733-9429(2001)127:1(6) (2001).
22. Meiburg, E. & Kneller, B. Turbidity currents and their deposits. *Annu. Rev. Fluid Mech.* **42**(1), 1. https://doi.org/10.1146/annurev-fluid-121108-145618 (2010).
23. Chamoun, S., De Cesare, G. & Schleiss, A. J. Managing reservoir sedimentation by venting turbidity currents: A review. *Int. J. Sediment Res.* **31**(3), 3. https://doi.org/10.1016/j.ijsrc.2016.06.001 (2016).
24. Chung, C.-C., Wu, P. L., Hsieh, S.-L., Lin, C.-P. & Wu, C.-H. Monitoring of Sediment Transport in a Reservoir using Time Domain Reflectometry. In *35th World Congress of the International-Association-for-Hydro-Environment-Engineering-and-Research (IAHR)* 6115–6127 (2013).

25. Chung, C.-C. & Wang, Y.-K. Practical assessment of real-time suspended sediment load monitoring using time domain reflectometry. *Water Resour. Res.* **58**(9), 9. https://doi.org/10.1029/2022WR032289 (2022).
26. Hage, S. *Turbidity current processes and products in the fjords of British Columbia (Canada)* [Phd, University of Southampton] (2019). https://eprints.soton.ac.uk/436679/
27. Wright, S. A. & Marineau, M. D. Turbidity current observations in a large reservoir following a major wildfire. *J. Hydraul. Eng.* **145**(8), 8. https://doi.org/10.1061/(ASCE)HY.1943-7900.0001611 (2019).
28. Lee, F. Z., Lai, J. S., Kantoush, S. A. & Sumi, T. Analysis of turbidity current plunging and floating woody debris in a reservoir during flood events. *J. Hydrol. Reg. Stud.* **56**(2024), 102027 (2024).
29. Baghalian, S. & Ghodsian, M. Experimental study on the effects of artificial bed roughness on turbidity currents over abrupt bed slope change. *Int. J. Sediment Res.* **35**(3), 3. https://doi.org/10.1016/j.ijsrc.2019.12.004 (2020).
30. Lee, H.-Y. & Yu, W.-S. Experimental study of reservoir turbidity current. *J. Hydraul. Eng.* **123**(6), 6. https://doi.org/10.1061/(ASCE)0733-9429(1997)123:6(520) (1997).
31. Miramontes, E. et al. Channel-levee evolution in combined contour current–turbidity current flows from flume-tank experiments. *Geology* **48**(4), 4. https://doi.org/10.1130/G47111.1 (2020).
32. Oehy, C. D., De Cesare, G. & Schleiss, A. J. Effect of inclined jet screen on turbidity current. *J. Hydraul. Res.* **48**(1), 1. https://doi.org/10.1080/00221680903566042 (2010).
33. An, R. & Li, J. Characteristic analysis of the plunging of turbidity currents. *J. Hydrodyn. Ser. B* **22**(2), 2. https://doi.org/10.1016/S1001-6058(09)60055-X (2010).
34. Choi, S.-U. Layer-averaged modeling of two-dimensional turbidity currents with a dissipative-Galerkin finite element method Part I: Formulation and application example. *J. Hydraul. Res.* **36**(3), 3. https://doi.org/10.1080/00221689809498623 (1998).
35. Huang, H., Imran, J. & Pirmez, C. numerical model of turbidity currents with a deforming bottom boundary. *J. Hydraul. Eng.* **131**(4), 4. https://doi.org/10.1061/(ASCE)0733-9429(2005)131:4(283) (2005).
36. Lai, Y. G., Huang, J. & Wu, K. Reservoir turbidity current modeling with a two-dimensional layer-averaged model. *J. Hydraul. Eng.* **141**(12), 12. https://doi.org/10.1061/(ASCE)HY.1943-7900.0001041 (2015).
37. Yi, Y.-K., Kim, Y.-D., Park, K.-Y. & Kim, W. Two dimensional numerical modeling of turbidity variation in Imha Reservoir. *KSCE J. Civ. Environ. Eng. Res.* **25**(4B), 4B (2005).
38. Imtiyaz, N., Lee, F. Z., Lin, G. F. & Lai, J. S. Modeling and analysis of turbidity currents in a reservoir with the dredged guiding channel. *KSCE J. Civ. Eng.* 1–13 (2024).
39. Hu, P., Cao, Z., Pender, G. & Tan, G. Numerical modelling of turbidity currents in the Xiaolangdi reservoir, Yellow River, China. *J. Hydrol.* **464**, 41–53 (2012).
40. Huang, C.-C., Lai, Y. G., Lai, J.-S. & Tan, Y.-C. Field and numerical modeling study of turbidity current in Shimen Reservoir during typhoon events. *J. Hydraul. Eng.* **145**(5), 05019003. https://doi.org/10.1061/(ASCE)HY.1943-7900.0001590 (2019).
41. Lee, F. Z. & Huynh Nguyen, N. L. Application of artificial countermeasures to enhance desilting efficiency in a reservoir under normal and extreme events. *J. Water Clim. Change* **15**(6), 2649 (2024).
42. Anari, R., Hotchkiss, R. H. & Langendoen, E. J. Elements for the successful computer simulation of sediment management strategies for reservoirs. *Water* **12**(3), 3. https://doi.org/10.3390/w12030714 (2020).
43. Chung, C.-C. & Lin, C.-P. High concentration suspended sediment measurements using time domain reflectometry. *J. Hydrol.* **401**(1–2), 134–144 (2011).
44. Hung, C.-C., Lai, J.-S. & Huang, C.-C. An efficient and economic desilitation strategy for reservoir sustainable development under the threat of extreme flooding threaten. *J. Water Clim. Change* **13**(3), 1257–1274 (2022).
45. Asthana, B. N. & Khare, D. Reservoir sedimentation. In *Recent Advances in Dam Engineering* (eds Asthana, B. N. & Khare, D.) 265–288 (Springer, 2022).
46. Fan, J. H. *Density currents and sedimentation engineering: Experiments and design* (China Water Resources and Hydropower Publishing House, 2011).
47. National Chiao Tung University. *Long-Term Monitoring of Sediment Transport in Shihmen Reservoir* (Water Resources Planning Institute, 2015).
48. Water Resources Planning Institute. *Study of Shihmen Reservoir upstream main river flood diversion and anti-silt project and hydraulic model test—Feasibility investigation and asses*. WRA, MOEA (2012).

Acknowledgements
The authors acknowledge the Northern Region Water Resources Office, Taiwan, for providing the essential data for analysis and simulation.

Author contributions
Cheng-Chia Huang generated the analyzed data and wrote the manuscript. Fong-Zuo Lee developed the principal countermeasure and approved the final manuscript.

Funding
A grant from the Ministry of Science and Technology (project number: NSTC 111-2625-M-035-007-MY3), the National Science and Technology Council (project number: NSTC 11-2221-E-005-092), and National Science and Technology Council (project number: NSTC 113-2221-E-005-027) provided financial support for this study.

Declarations

Competing interests
The authors declare no competing interests.

Additional information
Correspondence and requests for materials should be addressed to F.-Z.L.